ELSEVIER

Coordination Chemistry Reviews 226 (2002) 153–165

COORDINATION CHEMISTRY REVIEWS

www.elsevier.com/locate/ccr

Resonance Raman spectra and biological significance of high-valent iron(IV,V) porphyrins

Kazuo Nakamoto *

Department of Chemistry, Marquette University, P.O. Box 1881, Milwaukee, WI 53217-1881, USA

Received 28 March 2001; accepted 17 August 2001

Contents

Abstract . . . 153
1. Introduction . . . 153
2. Five-coordinate iron(IV) porphyrins . . . 154
3. Six-coordinate iron(IV) porphyrins . . . 157
4. Porphyrin π-cation radicals . . . 159
5. Five-coordinate iron(V) porphyrins . . . 161
6. Summary and prospects . . . 163
Acknowledgements . . . 164
References . . . 164

Abstract

Extensive research in the past decades has shown that nature relies on high-valent iron (IV,V) porphyrins in a number of enzyme-directed processes of heme proteins. For example, hydroxylation reaction catalyzed by cytochrome P450 involves an iron porphyrin intermediate which contains the oxoferryl moiety (Fe(IV)=O). Liver microsomal cytochrome P450-LM 3,4 is known to catalyze the transfer of a functionalized nitrogen atom intra- as well as inter-molecularly, and the proposed reaction cycle presumably involves a high-valent iron porphyrin intermediate which contains the nitrido-iron moiety(Fe(V)≡N). This review is focused on the biological significance of these high-valent iron(IV,V) porphyrins and their Fe(IV)=O and Fe(V)≡N stretching vibrations observed in resonance Raman spectra. © 2002 Published by Elsevier Science B.V.

Keywords: High-valent iron(IV,V) porphyrins; Resonance Raman spectra

1. Introduction

The most common oxidation states of iron in heme proteins are Fe(II) and Fe(III). For example, iron protoporphyrin which is the active site of myoglobin and hemoglobin is converted from the Fe(II) (five-coordinate, high spin) to the Fe(III) (six-coordinate, low spin) state upon oxygenation [1]. The Fe(IV) state is found in oxoferryl porphyrins (O=Fe(IV)(por)) which are involved in the enzymatic reactions of cytochrome P450, horseradish peroxidase (HRP) and related heme proteins, and their resonance Raman (RR) spectra have already been reviewed by several investigators [2–4]. However, the Fe(V) state is very rare; it is presumably involved as nitridoironporphyrins (N≡Fe(V)(por)) in

Abbreviations: OEP, octaethylporphyrin dianion; PPIXDME, protoporphyrin IX dimethylester dianion; TDCPP, tetrakis(2,6-dichlorophenyl)porphyrin dianion; TMP, tetramesitylporphyrin dianion; TMTMP, 2,7,12,17-tetramethyl-3,8,13,18-tetramesitylporphyrin dianion; TMPyP-2, tetrakis(2-*N*-methylpyridyl)porphyrin cation; TPFPP, tetrakis(pentafluorophenyl)porphyrin dianion; TpivPP, tetrakis(α,α,α,α-pivalamidophenyl)porphyrin dianion; TPP, tetraphenylporphyrin dianion; Salen, *N*,*N*′-ethylenebis(salicylideniminato) dianion; Cyclam, 1,4,8,11-tetraazacyclotetradecane; dias, *o*-phenylenebis(dimethylarsine); CAT, catalase; CcO, cytochrome *c* oxidase; CCP, cytochrome *c* peroxidase; CPO, chloroperoxidase; HRP, horseradish peroxidase; LPO, lactoperoxidase; MPO, myeloperoxidase; Mb, myoglobin.

* Tel./Fax: +1-414-352-6267.

E-mail address: knakamoto@worldnet.att.net (K. Nakamoto).

0010-8545/02/$ - see front matter © 2002 Published by Elsevier Science B.V.
PII: S0010-8545(01)00425-8

the functionalized nitrogen atom transfer reaction catalyzed by cytochrome P45O-LM3,4 [5]. This review is focused on the biological significance of these high-valent iron(IV,V) porphyrins and their Fe(IV)=O and Fe(V)≡N stretching vibrations observed in RR specra. In particular, RR spectra of nitridoiron(V) porphyrins are discussed in detail since they are not included or only mentioned briefly in the previous reviews. In most cases, RR spectra of model compounds were measured at low temperatures since they are highly unstable under ambient conditions.

2. Five-coordinate iron(IV) porphyrins

It has long been suggested that oxoferryl porphyrins (O=Fe(IV)(por)) are involved in the crucial stage of the reaction cycle of cytochrome P450 which catalyzes hydroxylation and epoxidation reactions of the substrates [6]. The first observation of the ν(Fe=O) (ν: stretching) vibration of oxoferryl porphyrin was somewhat serendipitous. In 1984, Bajdor and Nakamoto [7] were measuring the RR spectra of the dioxygen adduct, Fe(TPP)O_2, in O_2 matrices at $\sim$15 K using the apparatus shown in Fig. 1. (For the description of each of the components and experimental procedures, see their original papers [8,9].) Since the laser-heated miniature oven (enlarged in Fig. 1) requires only a very small quantity of the sample (typically 0.2 mg), it is ideal for measuring RR spectra of porphyrins containing expensive metal isotopes such as ^{54}Fe. Further, the use of a cylindrical lens provides a line focus on the sample surface, thus minimizing the thermal/photo-decomposition of the highly unstable species.

During their measurements (406.7 nm excitation, 1–2 mW) they noted that a new band emerged at 852 cm^{-1} and its intensity gradually increased whereas that of the $\nu(O_2)$ at 1195 and 1106 cm^{-1} (end-on and side-on type O_2 adducts, respectively [10]) decreased as a function of laser irradiation time, and that this photo-decomposition was completed after about 20 min. In order to determine the nature of the photo-product, the isotope shifts of the 852 cm^{-1} band were examined by ^{NA}Fe/^{54}Fe (^{NA}Fe: Fe in natural abundance, 92% pure ^{56}Fe) and $^{16}O_2/^{18}O_2$ substitutions. As seen in Fig. 2, the 852 cm^{-1} band was shifted $+4$ cm^{-1} by ^{NA}Fe/^{54}Fe and -34 cm^{-1} by $^{16}O_2/^{18}O_2$ substitutions. More importantly, similar experiments with an isotopically scrambled dioxygen ($^{16}O_2/^{16}O^{18}O/^{18}O_2 = 1/2/1$) produced two bands of equal intensities at 852 and 818 cm^{-1}. These results clearly indicate that the bands at 852 and 818 cm^{-1} are due to the ν(Fe=^{16}O) and ν(Fe=^{18}O), respectively, of oxoferryl porphyrin, O=Fe(TPP),which is formed via the O–O bond cleavage of Fe(TPP)O_2 on laser irradiation. A simple diatomic approximation gives a force constant of 5.32 mdyn $Å^{-1}$ for the Fe=O

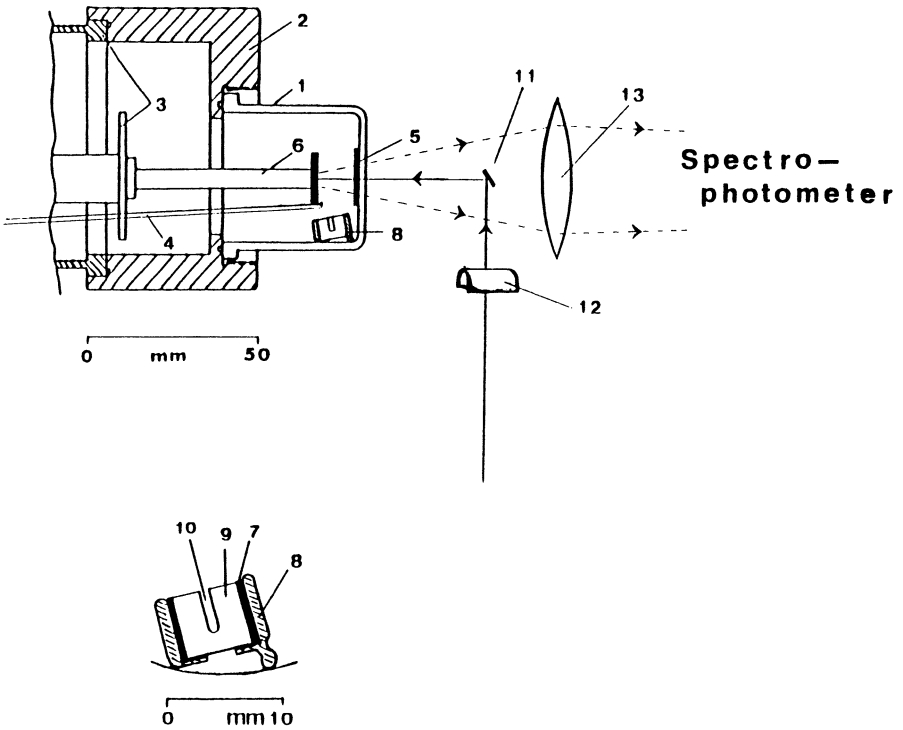

Fig. 1. Schematic drawing of matrix isolation apparatus used for RR measurements: 1, glass envelope; 2, aluminum sleeve; 3, closed-cycle helium refrigerator; 4, gas line; 5, steel screen; 6, cold tip; 7, aluminum radiation shield; 8, Pyrex cup; 9, spectroscopic-grade spark graphite rod; 10, Pyrex capillary tube with sample; 11, small mirror; 12, cylindrical lens; 13, collecting lens. The design of the miniature laser beam heated oven is seen in the enlarged diagram. Reproduced with permission from Ref. [9].

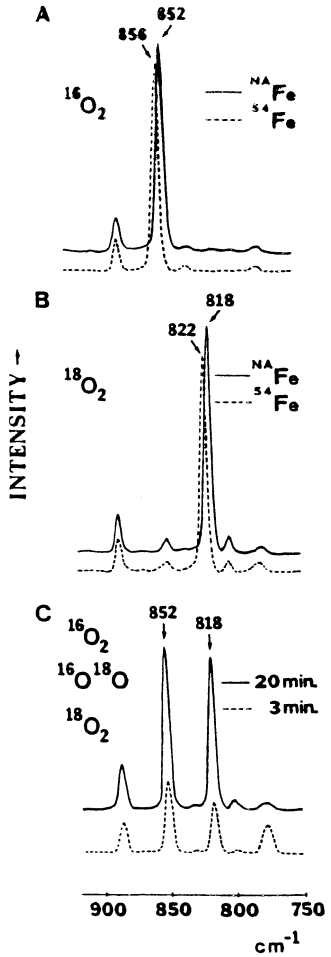

Fig. 2. RR spectra of Fe(TPP) co-condensed with O_2 at ~15 K (406.7 nm excitation, 1–2 mW). (A) ^{NA}Fe(TPP) with $^{16}O_2$(solid line) and ^{54}Fe(TPP) with $^{16}O_2$(broken line); (B) ^{NA}Fe(TPP) with $^{18}O_2$(solid line) and ^{54}Fe(TPP) with $^{18}O_2$ (broken line); and (C) ^{NA}Fe(TPP) with isotopically mixed dioxygen ($^{16}O_2/^{16}O^{18}O/^{18}O_2 = 1/2/1$). The solid and broken lines indicate the spectra obtained after 20 and 3 min of laser irradiation, respectively. Reproduced with permission from Ref. [7].

moiety which is much larger than that of the Fe–O–Fe bond of dimeric $(Fe(TPP))_2O$ (3.80 mdyn Å^{-1}). Proniewicz et al. [11] concluded that the Fe atom in O=Fe(TPP) is in the low-spin Fe(IV) state because the oxidation-state marker (ν_4) and the spin-state marker (ν_2) bands of TPP are observed at 1374 and 1575 cm^{-1}, respectively.

Fig. 3 shows the RR spectra of Fe(TPP-d_8)O_2 in an O_2 matrix (~30 K) measured as a function of the laser power [9]. The bands at 1195 ($\nu(O_2)$), 508 (ν(FeO)) and 345 cm^{-1} (δ(FeOO), δ: bending) belong to the end-on type dioxygen adduct while those at 1105 ($\nu(O_2)$) and 407 cm^{-1} (δ(FeOO)) are due to the side-on type dioxygen adduct. All these bands become weaker, whereas the two new bands at 853 and 815 cm^{-1} become stronger with an increasing laser power. Although the band at 853 cm^{-1} is due to the ν(Fe=O) of O=Fe(TPP-d_8), the nature of the latter at 815 cm^{-1} is not immediately obvious. This band must also be assigned to the ν(Fe=O) vibration since both bands give exactly the same magnitude of isotopic shift (35 cm^{-1}) by $^{16}O_2/^{18}O_2$ substitution. However, plots of the intensity versus laser irradiation time reveal their differences. As seen in Fig. 4, the intensity of the 815 cm^{-1} band rapidly reaches a maximum and then decreases exponentially with time, whereas that of the 853 cm^{-1} band increases monotonically with time. Based on these observations, the 815 cm^{-1} band was attributed to the ν(Fe=O) of the oxoferryl porphyrin π-cation radical which was formed via the mechanism shown in Fig. 5. Here, the electronic structure of the Fe–O_2 moiety is expressed by two resonance structures. First, the homolytic cleavage of the O–O bond by laser irradiation produces an oxoferryl porphyrin π-cation radical and an oxygen

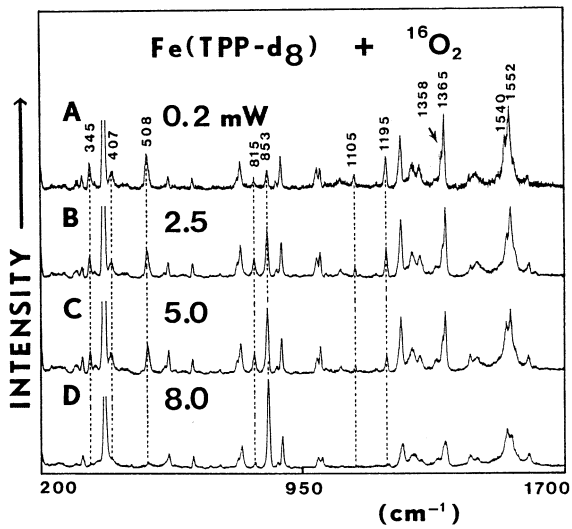

Fig. 3. RR spectra of Fe(TPP-d_8) co-condensed with $^{16}O_2$ at ~30 K (406.7 nm excitation). (A) 0.2; (B) 2.5; (C) 5.0; and (D) 8.0 mW. Reproduced with permission from Ref. [9].

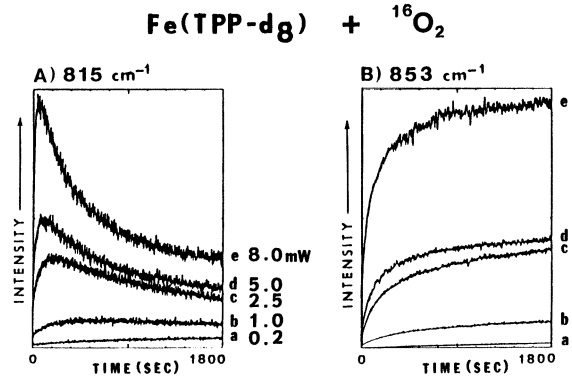

Fig. 4. Relative intensity vs. time of laser irradiation for the two ν(Fe=O) vibrations at 815 (A) and 853 cm^{-1}(B) observed during the photolysis of Fe(TPP-d_8) $^{16}O_2$ at ~30 K (406.7 nm excitation). Laser powers used are indicated for each trace. Reproduced with permission from Ref. [9].

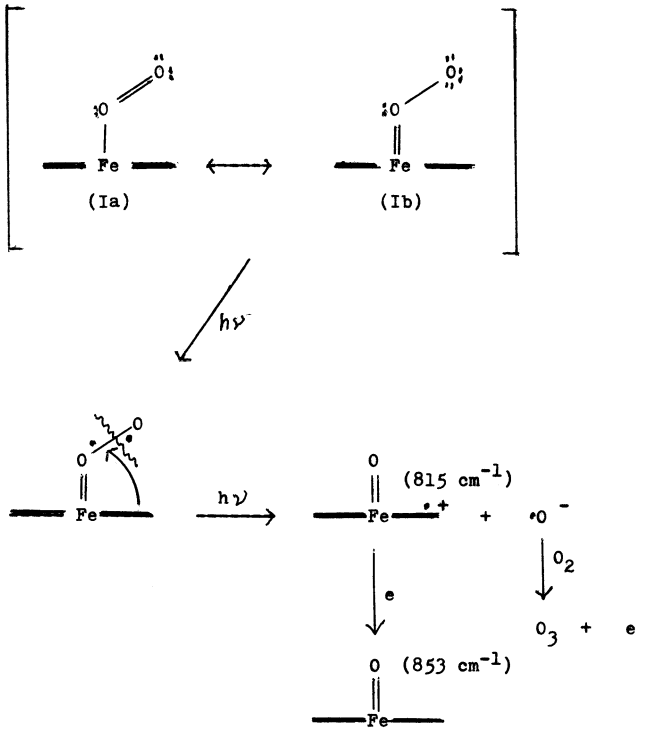

Fig. 5. Proposed mechanism for the formation of π-cation radical and non-radical oxy-ferryl porphyrins in O_2 matrices. Reproduced with permission from Ref. [9].

anion radical. Secondly, the latter reacts readily with O_2 in an O_2 matrix to form ozone (O_3) and an electron that neutralizes the porphyrin π-cation radical to give non-radical oxoferryl porphyrin. As discussed in Section 4, oxoferryl porphyrin π-cation radical is regarded as a model compound of HRP-I.

Cytochrome P450 is known to catalyze the epoxidation reaction of an olefin such as ethylene. Weselucha-Birczynska et al. [12] measured the RR spectra of the co-condensation products of Fe(TPP) with O_2/C_2H_4 to determine the structure of the intermediate species involved in this epoxidation reaction. Two bands at 850 and 804 cm^{-1} in Fig. 6A can be assigned to the ν(Fe=O) of free O=Fe(TPP) and O=Fe(TPP) bonded to ethylene, respectively, because they are shifted by 35 cm^{-1} (to 815 and 769 cm^{-1}, respectively) by $^{16}O_2/^{18}O_2$ substitution (Fig. 6B). On $^{12}C_2H_4/^{13}C_2H_4$ substitution (Fig. 6C), however, the band at 804 cm^{-1} is shifted to 801 cm^{-1} whereas that at 850 cm^{-1} remains unshifted. Further, the $^{18}O_2/C_2H_4$ experiment (Fig. 6B and B′) shows that the intensity of the 815 cm^{-1} band (free ^{18}O=Fe(TPP)) decreases, whereas that of the 769 cm^{-1} band (^{18}O=Fe(TPP) bonded to ethylene) increases, when the matrix is warmed from 20 to 25 K. This result suggests that the formation of the bonded species is accelerated by an increased diffusion of both components on warming the matrix. A rather small shift (3 cm^{-1}) of the 804 cm^{-1} band by $^{12}C_2H_4/^{13}C_2H_4$ substitution implies that species IIa is more likely than IIb between the two intermediates shown in Fig. 7.

Five-coordinate oxoferryl porphyrins can also be prepared in solution at low temperatures. In general, the oxidation reaction of iron porphyrins (PFe) proceeds through the following intermediates [13,14]

$$\underset{A}{PFe} \xrightarrow{O_2} \underset{B}{PFeO_2} \xrightarrow{PFe} \underset{C}{PFe{-}O{-}O{-}FeP} \xrightarrow{\text{warming}} \underset{D}{PFe{=}O} \xrightarrow{PFe} \underset{E}{PFe{-}O{-}FeP}$$

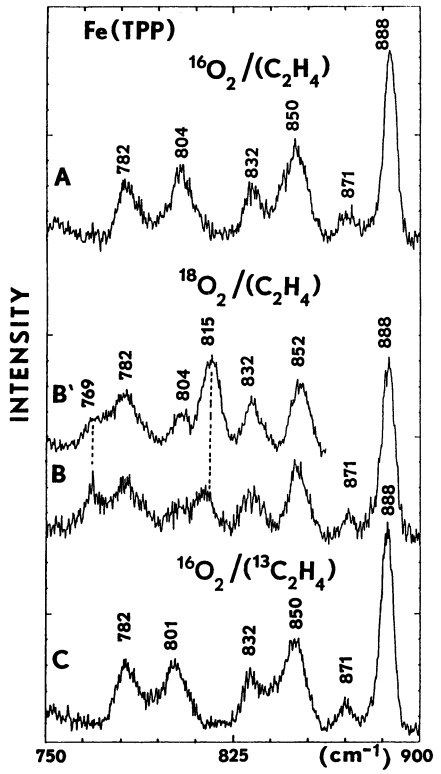

Fig. 6. RR spectra of co-condensation products of Fe(TPP) with O_2/C_2H_4 (1; 1). (A) Fe(TPP) with $^{16}O_2/C_2H_4$ at 25 K; (B) Fe(TPP) with $^{18}O_2/C_2H_4$ at 25 K; (B′) Fe(TPP) with $^{18}O_2/C_2H_4$ at 20 K; and (C) Fe(TPP) with $^{16}O_2/^{13}C_2H_4$ at 25 K. Reproduced with permission from Ref. [12].

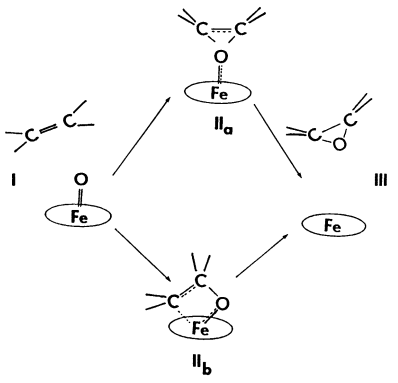

Fig. 7. Structures of the two possible intermediates in epoxidation reaction of ethylene catalyzed by oxo-ferryl porphyrin. Reproduced with permission from Ref. [12].

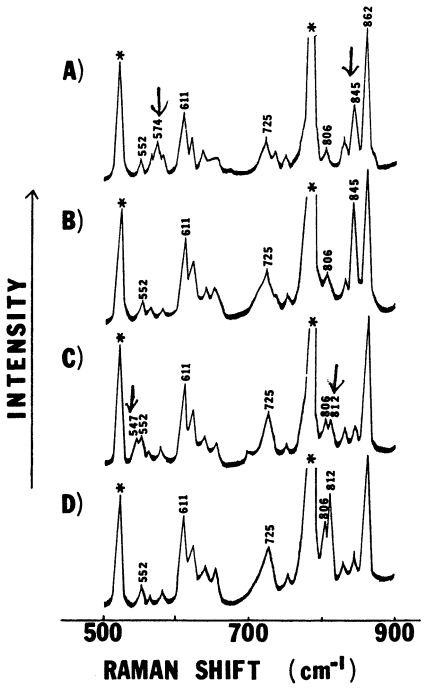

Fig. 8. RR spectra of Fe(TMP) in toluene saturated with O_2. (A) $^{16}O_2$, ~ -78 °C; (B) $^{16}O_2$, ~ -46 °C; (C) $^{18}O_2$, ~ -78 °C; and (D) $^{18}O_2$, ~ -46 °C. Reproduced with permission from Ref. [15].

Fig. 8A and B shows the RR spectra of Fe(TMP) in toluene saturated with $^{16}O_2$ and measured at ~ -78 and ~ -46 °C, respectively, as obtained by Paeng et al. [15]. The most significant features of these spectra are the marked enhancement of the 845 cm^{-1} band and the complete disappearance of the 574 cm^{-1} band when the temperature is raised from ~ -78 to ~ -46 °C. Similar trends are observed for the solution saturated with $^{18}O_2$, although the bands at 845 and 574 cm^{-1} are now shifted to 812 and 547 cm^{-1}, respectively, due to $^{16}O_2/^{18}O_2$ substitution (Fig. 8C and D). The bands at 845 and 812 cm^{-1} are readily attributed to the ν(Fe=O) of O=Fe(TMP). On the other hand, the band at 574 cm^{-1}, which is shifted to 547 cm^{-1} by $^{16}O_2/^{18}O_2$ substitution, is assigned to the symmetric ν(Fe–O) vibration of (TMP)Fe–O–O–Fe(TMP) which is presumably centrosymmetric. The RR spectra of these solutions were measured by using the mini-bulb technique that requires only a small volume of the solution (less than 0.4 ml) [16]. The ν(Fe=O) vibrations in solution were also measured by other workers. Mizutani et al. [17] observed the ν(Fe=O) of O=Fe(TMP) at 843 cm^{-1} in toluene-d_8 at -70 °C, and Czarnecki et al. [18] located the ν(Fe=O) of O=Fe(TMTMP) at 845 cm^{-1} in toluene at -70 °C. Czernuszewicz and Macor [19] generated O=Fe(TMP) by the electrooxidation of Fe(TMP)(OH) in CH_2Cl_2 solution at -40 °C, and observed its ν(Fe=O) at 841 cm^{-1}. In special circumstances, the ν(Fe=O) can be measured in aqueous solution at room temperature (r.t.). For example, Shantha and Verma [20] were able to observe the ν(Fe=O) of O=Fe(TPP) at 843 cm^{-1} via photolysis (441.6 nm, He–Cd laser) of the μ-oxo dimer, $(Fe(TPP))_2O$, in an aqueous alkaline TX-100 detergent micelle at r.t.

Table 1 summarizes the ν(Fe=O) frequencies and the experimental conditions reported thus far. In most cases, the 406.7 nm line of a Kr-ion laser was used for RR excitation, because the Fe←O charge-transfer band is located in the Soret region. However, the 457.9 nm line of an Ar-ion laser was chosen for O=Fe(salen) because its Fe←O charge-transfer transition is located near 460 nm [11].

3. Six-coordinate iron(IV) porphyrins

Oxoferryl porphyrins containing base ligands (B) at the axial position *trans* to the Fe=O group, O=Fe(por)B, are important as model compounds of HRP-II and related heme proteins. It is technically difficult, however, to prepare these six-coordinate model compounds in O_2 matrices because the base ligand in

Table 1
ν(Fe=O) frequencies of five-coordinate oxo-ferryl porphyrins

Compound	ν(Fe=O) (cm^{-1})	ν (cm^{-1}) [a]	Experimental conditions	References
O=Fe(TPP)	852	34	O_2 mat, ~15 K	[7,11]
O=Fe(TPP-d_8)	853	35	O_2 mat, ~30 K	[9]
O=Fe(OEP)	853	35	O_2 mat, ~30 K	[9,11]
O=Fe(TMP)	854	35	O_2 mat, ~30 K	[9]
O=Fe(TPFPP)	861	36	O_2 mat, ~30 K	[9]
O=Fe(salen)	851	35	O_2mat, ~15 K	[11]
O=Fe(TMP)	845	33	Toluene, −78 °C	[15]
O=Fe(TMP)	843	36	Toluene, −70 °C	[17]
O=Fe(TMTMP)	845	36	Toluene, −70 °C	[18]
O=Fe(TMP)	841	36	CH_2Cl_2, −40 °C	[19]
O=Fe(TPP)	843	–	Micelle, r, t	[20]

[a] Isotope shift by the $^{16}O/^{18}O$ substitution.

Table 2
ν(Fe=O) frequencies of six-coordinate oxo-ferryl porphyrins

Compound	ν(Fe=O) (cm^{-1}) [a]	Experimental conditions [b]	References
O=Fe(T_{piv}PP)(THF)	829(37)	THF, −50 °C, 454.5 nm	[22]
O=Fe(T_{piv}PP)(1-MeIm)	807	THF, −50 °C, 454.5 nm	[22]
O=Fe(TPP)(*N*-MeIm)	820	Toluene, −120 °C, 406.7 nm	[23]
O=Fe(OEP)(*N*-MeIm)	820	Toluene, −120 °C, 406.7 nm	[23]
O=Fe(PPIXDME)(*N*-MeIm)	820(36)	Toluene, −120 °C,406.7 nm	[23,24]
O=Fe(TDCPP)(THF)	841	THF, −50 °C, 457.9 nm	[25]
O=Fe(TDCPP)(DMF)	828	DMF, −50 °C, 457.9 nm	[25]
O=Fe(TDCPP)(*N*-MeIm)	818	THF, −50 °C, 457.9 nm	[25]
$[O=Fe(TMPyP\text{-}2)(OH)]^{3+}$	763(29)	aq. pH 12, 0 °C, 441.6 nm	[26]

[a] The number in the brackets indicates the isotope shift by the $^{16}O/^{18}O$ substitution.
[b] The solvent, temperature and exciting wavelength used.

Table 3
ν(Fe=O) frequencies of heme proteins

Compounds	ν(Fe=O) (cm^{-1}) [a]	Experimental conditions [b]	References
HRP-II(isozyme C)	787(34)	12	[27]
HRP-II(isozyme C)	774(34)	7.0	[28]
	786	11.2	
HRP-II(isozyme A)	775(34)	5.3	[29]
HRP-II(isozyme A)	779(36)	7	[30]
HRP-II(isozyme B,C)	775(28)	6.9	[31]
	788(31)	10.0	
CCP-ES	767(40)	4–11	[32,33]
MPO-II	782(35)	10.7, 5 °C	[34]
LPO-II	745(33)	6–10	[33]
CPO-I	790(34)	3.5, 363.8 nm	[35,36]
CAT-II	775(29)	7.5, 4 °C	[37]
	786(30)	8.9, 4 °C	
CcO('607 nm' form)	804(39)	8.5	[38]
CcO('580 nm' form)	785(35)	8.5	
Cytochrome *d* [c]	815(46)	5.7, 5 °C, 647.1 nm	[39]
Oxo-ferryl Mb	797(26)	8.6, 20 °C	[40]

[a] The number in the brackets indicates the isotope shift by the $^{16}O_2/^{18}O_2$ substitution.
[b] The experimental conditions are shown in the order of pH, temperature and exciting wavelength. If not shown, the spectra were measured at r.t. using 406.7 nm excitation.
[c] Chlorin-containing heme.

Fe(por)B tends to dissociate during the process of vaporization in vacuo. Thus, all the results shown below were obtained in solution at low temperatures.

Six-coordinate oxoferryl porphyrins can be formed in toluene by the following reaction [21–24]:

$$(por)Fe\text{–}O\text{–}O\text{–}Fe(por) \xrightarrow{2B} 2O{=}Fe(por)B$$

or by the oxidation of Fe(por)(OH) with *m*-chloroperoxybenzoic acid (*m*-CPBA) in THF or DMF solution [25]. Table 2 lists the observed ν(Fe=O) frequencies of six-coordinate model compounds together with the experimental conditions employed. In general, these frequencies are lower than those of the five-coordinate species discussed earlier owing to the *trans* effect of the axial base ligand (B) [11]. As expected, the stronger the base, the lower the ν(Fe=O). This trend is clearly seen in the O=Fe(TDCPP)B and O=Fe(T_{piv}PP)B series. The ν(Fe=O) of the $[O=Fe(TMPyP\text{-}2)(OH)]^{3+}$ ion is exceptionally low and close to that of HRP-II (Table 3). This may be attributed to several factors including the strong *trans*-effect of the OH^- group and 4+ charges on the 2-*N*-methylpyridyl groups surrounding the Fe=O moiety.

Shortly after Bajdor and Nakamoto [7] observed the ν(Fe=O) of O=Fe(TPP) in O_2 matrices, two research groups, Kitagawa et al. [27–29] and Terner et al. [30,31], were able to locate the ν(Fe=O) of HRP-II independently and almost simultaneously. Horseradish peroxidase (HRP) catalyzes the oxidation of a substrate (AH_2) by H_2O_2 via the following reaction cycle that involves the two intermediates, HRP-I and HRP-II.

$$HRP(ferric) + H_2O_2 \rightarrow HRP\text{-}I + H_2O$$

$$HRP\text{-}I + AH_2 \rightarrow HRP\text{-}II + AH$$

$$\text{HRP-II} + \text{AH} \rightarrow \text{HRP(ferric)} + \text{A} + \text{H}_2\text{O}$$

Thus, HRP-I (green) and HRP-II (red) have oxidation states higher than the resting state (Fe(III)) by two and one oxidizing equivalents, respectively. When HRP and H_2O_2 are mixed in 1:1 molar ratio, HRP-I is produced first and then rapidly converted to HRP-II. Since the latter is stable for 2–3 min, it is possible to measure the RR spectrum using an optical multichannel analyzer. The ν(Fe=O) of HRP-II (isozyme C) is at 787 cm^{-1} in an alkaline solution (pH 11) but at 774 cm^{-1} in a neutral solution. This lowering of the ν(Fe=O) in neutral solution was attributed to the effect of hydrogen bonding to the distal imidazole (Fig. 9). As shown in Table 3, the same pH effect is seen for CAT-II. In the high frequency region, HRP-II exhibits the oxidation-state marker band (ν_4) at 1378 cm^{-1} and the spin-state marker band (ν_2) at 1582 cm^{-1}, thus confirming the low-spin Fe(IV) state of HRP-II [41].

Table 3 also lists the ν(Fe=O) frequencies of other heme proteins. Their ν(Fe=O) frequencies are scattered in a wide range from 815 cm^{-1} (cytochrome *d*) to 745 cm^{-1} (LPO-II). In general, these frequencies are lower than those of the model compounds listed in Table 2. This is due to several factors; the *trans* effect of the proximal ligand, hydrogen-bonding interaction with the distal amino acid residue, polarization effect of the heme cavity, and their combinations. Among them, the *trans* effect is expected to be most significant as observed for the six-coordinate model compounds (Table 2). Most of the axial ligands in the heme proteins listed in Table 3 are the proximal histidyl imidazole residues (Fe–N bonding) except for CAT-II, which is known to be the tyrosine residue (Fe–O^- bonding). Yet, their ν(Fe=O) frequencies are surprisingly similar. Thus, the *trans* effect does not seem to play the major role in this case. As stated earlier, it is of particular interest to observe the ν(Fe=O) vibration of the oxoferryl porphyrin intermediate in the reaction cycle of cytochrome P450 containing the cysteinyl residue as the axial ligand (Fe–S^- bonding). To date, no reports are available on the ν(Fe=O) of this enzymatic intermediate although the ν(Fe=O) of CPO-I having the same axial ligand was observed at 790 cm^{-1} [35,36].

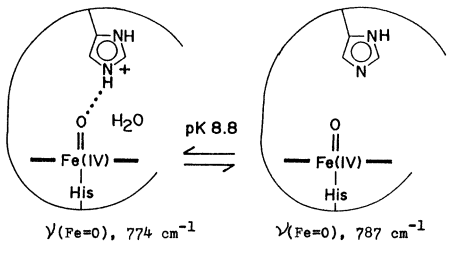

Fig. 9. Schematic diagram to explain the pH dependence of the ν(Fe=O) in HRP.

4. Porphyrin π-cation radicals

Porphyrin π-cation radicals are highly photo-labile. As discussed in Section 2, Proniewicz et al. [9] observed a new band at 815 cm^{-1} during the photolysis of Fe(TPP-d_8)O_2 in O_2 matrices and assigned it to the ν(Fe=O) of the five-coordinate π-cation radical intermediate, O=Fe(TPP-$d_8^{+\bullet}$). This frequency is 38 cm^{-1} lower than that of the corresponding non-radical, O=Fe(TPP-d_8) (853 cm^{-1}). Following the pioneering work by Groves et al. [41], Kincaid et al. [42] generated O=Fe($TMP^{+\bullet}$) by the reaction of Fe(TMP)Cl with *m*-CPBA in CH_2Cl_2 solution at -78 °C, and observed the ν(Fe=O) of O=Fe($TMP^{+\bullet}$) at 802 cm^{-1}. In this case, the ν(Fe=O) has shifted by -41 cm^{-1} in going from O=Fe(TMP) (843 cm^{-1}) to its radical cation. Earlier, Hashimoto et al. [43] had carried out similar experiments using a mixed solvent, CH_2Cl_2–CH_3OH, and observed the ν(Fe=O) of the same π-cation radical at 828 cm^{-1}. Although these two results appeared contradictory, ensued extensive research by both groups revealed that the 828 cm^{-1} band observed by the latter workers is not due to a photoproduct as once suggested [42], but due to the six-coordinate species [O=Fe($TMP^{+\bullet}$) (CH_3OH)]$^+$ [44]. Later, the 802 cm^{-1} band reported by the former workers was reassigned to the six-coordinate species with Cl^- as the axial ligand [45].

The *trans* effect on the ν(Fe=O) in the six-coordinate species, O=Fe($TMP^{+\bullet}$)L, was first noted by Hashimoto et al. [44] who observed that the ν(Fe=O) is shifted from 828 to 801 cm^{-1} when L is changed from CH_3OH to *m*-CPBA. Czarnecki et al. [45] carried out a more extensive investigation using a variety of axial ligands (L). Table 4 lists the ν(Fe=O) of porphyrin π-cation radicals reported so far. It is seen that the ν(Fe=O) values are near 835 cm^{-1} for L = ClO_4^- and $CF_3SO_3^-$ and near 800 cm^{-1} for L = F^-, Cl^- and *m*-$CPBA^-$. These results clearly indicate that the electron-donating capabilities of the latter group are much greater than those of the former group.

When one electron is lost from the porphyrin π-orbital, two types of π-cation radicals, $^2A_{1u}$ and $^2A_{2u}$, can be formed. Fig. 10 illustrates the atomic p_z orbitals of magnesium porphine in the two highest occupied molecular orbitals. The circle sizes are proportional to the coefficients of the atomic orbitals, and the open circles represent negative signs of the upper lobes of the p_z orbitals [46]. It is seen that the C_β–C_β bond is anti-bonding in the a_{1u} orbital whereas it is bonding in the a_{2u} orbital. The ν_2 band of a metalloporphyrin contains a contribution from the $\nu(C_\beta–C_\beta)$ mode. Thus, ν_2 is expected to downshift in an $^2A_{2u}$ radical and upshift in an $^2A_{1u}$ radical. A similar trend holds for ν_4 which is a symmetric pyrrole ring vibration. Kincaid et al. [42] concluded that the six-coordinate O=Fe($TMP^{+\bullet}$)

Table 4
ν(Fe=O) frequencies of porphyrin π-cation radicals

Compound	ν(Fe=O) (cm^{-1}) [a]	Experimental conditions [b]	References
O=Fe($TPP^{+\bullet}$)	815(35)	O_2 matrix, ~30 K	[9]
O=Fe($TMP^{+\bullet}$)	802(35)	CH_2Cl_2, −78 °C	[42]
O=Fe($TMP^{+\bullet}$)(CH_3OH)	828(36)	$CH_2Cl_2+CH_3OH$, −80 °C	[43]
O=Fe($TMP^{+\bullet}$)(*m*-CBA^-) [c]	801(37)	CH_2Cl_2, −80 °C	[44]
O=Fe($TMP^{+\bullet}$)L		CH_2Cl_2, −80 °C	[45]
L = CH_3OH	831		
ClO_4^-	835		
$CF_3SO_3^-$	834		
m-CBA^-	806		
Cl^-	801		
F^-	801		

[a] The number in the brackets indicates the isotope shift by the $^{16}O/^{18}O$ substitution.
[b] The exciting line is 406.7 nm in all cases.
[c] *m*-Chlorobenzoate ion.

(vide supra) belongs to the $^2A_{2u}$ type since both ν_2 and ν_4 are downshifted by ~30 and ~10 cm^{-1}, respectively, compared with the corresponding non-radical species. Hashimoto et al. [44] also reached the same conclusion for the six-coordinate π-cation radical containing CH_3OH as the axial ligand. Previously, Fujii and Ichikawa [47] inferred from the NMR data that O=Fe(TMTMP) forms an $^2A_{1u}$ type π-cation radical on oxidation. The RR studies by Ayougou et al. [48] also reached the same conclusion. Czarnecki et al. [18] located the ν(Fe=O) of [O=Fe($TMTMP^{+\bullet}$)] (ClO_4^-) at 833 cm^{-1} which is virtually identical with that of [O=Fe($TMP^{+\bullet}$)](ClO_4^-) (835 cm^{-1}). Since the latter belongs to the $^2A_{2u}$ type, these results indicate that the ν(Fe=O) of the oxoferryl porphyrin π-cation radicals are rather insensitive to the radical type. In some cases, electronic states of iron porphyrin π-cation radical cations can be explained as the admixture of the a_{1u} and a_{2u} character [49].

It has long been recognized that HRP-I is the π-cation radical produced by the one-electron oxidation of HRP-II. During the period from 1987 to 1992, five research groups [50–54] reported the RR spectrum of HRP-I. However, their results caused confusion and controversy because HRP-I is extremely photolabile upon laser irradiation. Since the formation of HRP-I can be confirmed by electronic spectroscopy, Ogura and Kitagawa [50] constructed a novel device to measure the RR (406.7 nm excitation) and electronic absorption spectra simultaneously. However, they could not distinguish the two radical types since no prominent shifts were observed between the RR peaks of HRP-I and HRP-II in the 1700–1200 cm^{-1} region. According to these workers, one likely reason for this similarity is that a clear cation radical state as seen in the model compounds does not exist for HRP-I because electrons are delocalized through the metal and the axial ligands. On the other hand, Oertling and Babcock [51] measured the RR spectrum (390 nm excitation, 10 ns pulses) of HRP-I prepared by the rapid mixing and flow sample techniques, and also noted the similarity in RR spectra between HRP-I (pH 7.0) and HRP-II (pH 10.8). In the low-frequency region, the former exhibited the ν(Fe=O) at 791 cm^{-1} which is almost identical to that of the latter (787 cm^{-1}). These workers considered the two possible interpretations of this similarity; one is the extensive electron delocalization mentioned above [50], and the other is the conversion of HRP-I to HRP-I* via rapid and efficient photo-induced electron transfer. In the latter, one electron is transferred from a nearby amino acid residue to the porphyrin cation radical, resulting in a ring-neutral oxoferryl species similar to HRP-II.

Paeng and Kincaid [52] used a micro-droplet sample device to reduce the sample-residence time in the laser beam (406.7 nm excitation) to less than 5 μs, and assigned the ν(Fe=O) of HRP-I at 737 cm^{-1} which is 39 cm^{-1} lower than that of HRP-II. Their spectrum in the high frequency region suggested the $^2A_{2u}$ formulation. Using a similar device, Chuang and Van Wart [53]

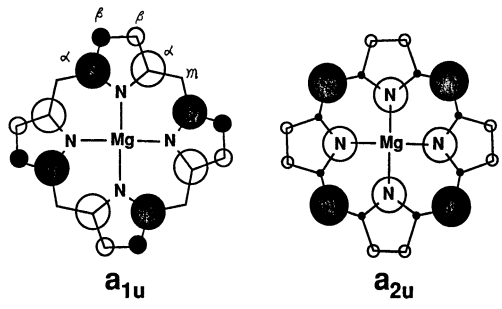

Fig. 10. The atomic orbital (AO) structure of Mg porphyrin in the two highest occupied orbitals. The circle sizes are approximately proportional to the AO coefficients. The open circles represent negative signs of the upper lobes of the p_z atomic orbitals. Reproduced with permission from Ref. [46].

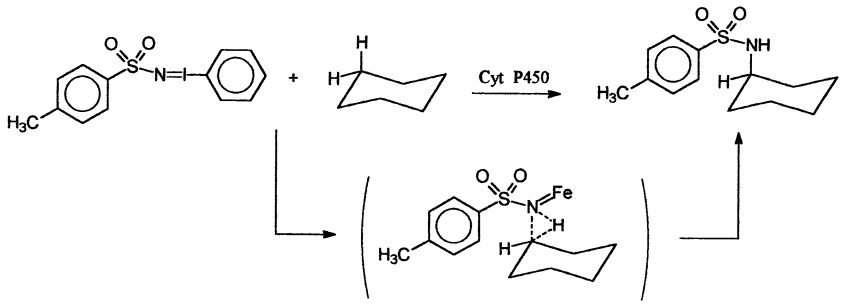

Fig. 11. Intermolecular functionalized nitrogen atom transfer reaction catalyzed by cytochrome P450-LM 3,4.

observed a band at 721 cm^{-1} which they assigned to the ν(Fe=O) of HRP-I. Palaniappan and Terner [54] employed the exciting lines near 350 nm and obtained a 'unique spectrum' distinctly different from that of HRP-II. Their spectrum in the high frequency region gave marker mode frequencies that are consistent with the $^2A_{1u}$ formulation. In 1996, Kincaid and co-workers [55] measured the RR spectrum of HRP-I with 356.4 nm excitation by changing the laser power. They found that, with low laser power (1 mW), the conversion of HRP-I to HRP-I* and/or HRP (resting state) [54] is minimized and concluded that the RR spectrum obtained with near UV excitation is that of HRP-I as originally suggested by Palaniappan and Terner [54]. In the low frequency region, the ν(Fe=O) was observed at $\sim$790 cm^{-1} (pH 7.5) which is similar to that reported by Oertling and Babcock [51], but markedly different from their previous value (737 cm^{-1}) [52], which is too low to be attributed to a HRP-I* photoproduct. With high laser power (5–25 mW), their RR spectra in the high frequency region show that HRP-I is converted to a HRP-II-like photoproduct. These results essentially confirmed the validity of the previous work by Palaniappan and Terner [54].

5. Five-coordinate iron(V) porphyrins

In 1985, Svastits et al. [5] reported that rabbit liver microsomal cytochrome P450-LM 3,4 isozyme catalyzes the functionalized nitrogen atom transfer as shown in Fig. 11. This reaction may involve nitridoiron(V) porphyrin as an intermediate since analogous nitridomanganese(V) porphyrin is known to catalyze the oxidative amination of hydrocarbons [56]. Although nitrido porphyrins of Mn(V) and Cr(V) are stable and can be isolated under ambient conditions, the corresponding Fe(V) porphyrins had not been known until Wagner and Nakamoto [57,58] prepared them via laser photolysis of the corresponding azido complexes at $\sim$30 K:

$$N_3\text{–Fe(por)} \xrightarrow{h\nu} N{\equiv}\text{Fe(por)} + N_2$$

The photolysis and subsequent RR measurements were carried out using the apparatus shown in Fig. 1. In this case, thin films of the azido complexes were prepared on the surface of the cold tip, and the RR spectra were measured at $\sim$30 K using exciting lines in the 520–400 nm region.

Fig. 12 shows the RR spectra (488.0 nm excitation) of N_3–Fe(OEP) as a function of the laser power used [58]. The bands at 418, 628 and 831 cm^{-1} (trace a) can be assigned to the ν(Fe–N_3), $\delta(N_3^-)$ and 2ν(Fe–N_3), respectively, of N_3–Fe(OEP) since they are shifted by $^{54}Fe/^{56}Fe$ and $^{14}N/^{15}N$ substitutions [59]. As the laser power is increased from 5 to 100 mW (traces b–f), these three bands together with those at 701 and 341 cm^{-1} become weaker, whereas the bands at 876, 752 and 673 cm^{-1} become stronger. These changes are completed after continued laser irradiation with 100 mW for 10 min (trace g).

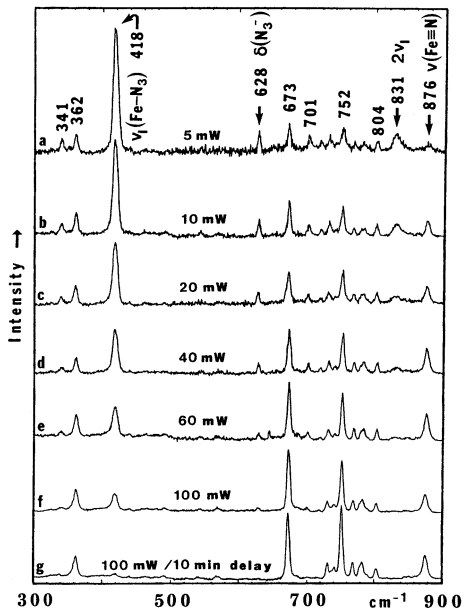

Fig. 12. RR spectra of a thin film of N_3–Fe(OEP) at $\sim$30 K, 488 nm excitation. The laser power used is indicated for each trace. Trace g was obtained after 10 min preirradiation with 488.0 nm, 100 mW. Reproduced with permission from Ref. [58].

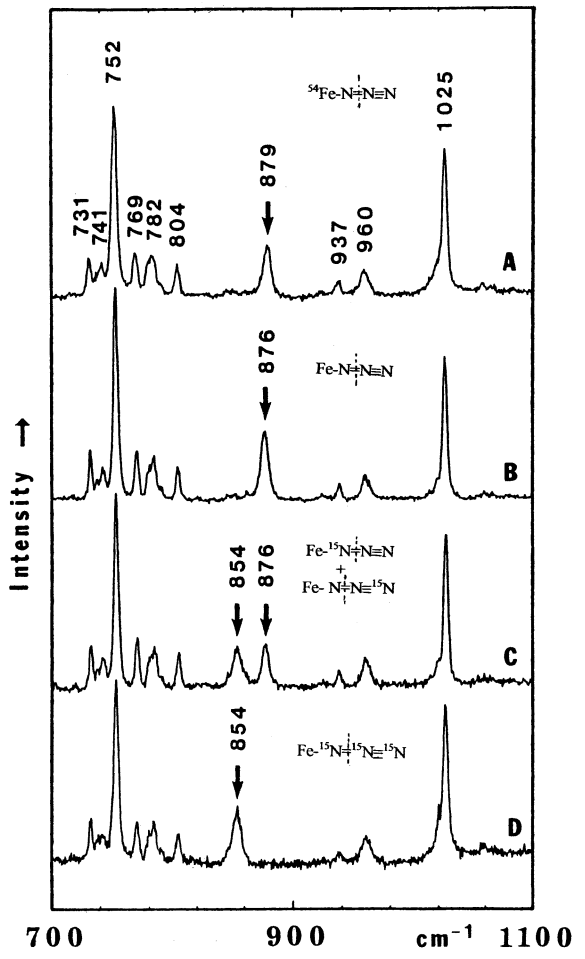

Fig. 13. RR spectra of the photolysis products of N_3–Fe(OEP), thin films, at ~30 K, 488.0 nm, 60 mW. The structures of isotopically substituted azido groups are shown for each trace. Reproduced with permission from Ref. [58].

Fig. 13 compares the RR spectra of photoproducts of N_3–Fe(OEP) and its isotopically substituted analogs. The 876 cm^{-1} band (trace B) is upshifted to 879 cm^{-1} (trace A) by $^{NA}Fe/^{54}Fe$ substitution and downshifted to 854 cm^{-1} (trace D) by $^{14}N/^{15}N$ substitution. More importantly, a 1:1 mixture of the Fe–^{15}N=N≡N and Fe–N=N≡^{15}N complexes (prepared by using the $N_2^{15}N$ azido ion) exhibits two bands of equal intensities at 876 and 854 cm^{-1} (trace C). These results provide definitive evidence that the Fe–N=N≡N moiety is cleaved at the N=N linkage to yield N≡Fe(OEP) and N_2 and that the 876 cm^{-1} band is due to the ν(Fe≡N) of the nitrido complex, N≡Fe(OEP). The observed shifts of $+3$ cm^{-1} by $^{NA}Fe/^{54}Fe$ substitution and -23 cm^{-1} by $^{14}N/^{15}N$ substitution are in good agreement with the theoretical values expected for a Fe≡N diatomic harmonic oscillator. Similar isotopic shift behavior was observed for the first overtone of the ν(Fe≡N) at 1741 cm^{-1}. In addition, the nitrido complex exhibits three strong OEP vibrations at 1025, 752 and 673 cm^{-1}.

In the high frequency region, N≡Fe(OEP) exhibits the oxidation-state marker band (ν_4) at 1384 cm^{-1} which is higher than that of O=Fe(IV) (OEP) (1379 cm^{-1}), thus supporting the Fe(V) formulation. However, the distinction between the low-spin state, $(d_{xy})^2(d_{xz})^1$, and the high-spin state, $(d_{xy})^1(d_{xz})^1(d_{yz})^1$, cannot be made based on the spin-state marker bands since the core sizes of both configurations are similar. It was suggested [58] that N≡Fe(OEP) is probably of high-spin because it is isoelectronic with the known high-spin complex, O=Mn(IV)(TPP). Further, the Fe≡N stretching force constant (5.07 mdyn $Å^{-1}$) is only slightly larger than that of $(Fe(OEP))_2N$ (4.8 mdyn $Å^{-1}$) in which the Fe atom is of low spin and its formal oxidation state is $+3.5$, and is slightly smaller than that of the Fe=O bond (5.32 mdyn $Å^{-1}$) of the oxoferryl porphyrin in which the Fe(IV) atom is of low spin. As will be discussed in the next section, these results can be explained by assuming that N≡Fe(OEP) takes the high-spin $(d_{xy})^1(d_{xz})^1(d_{yz})^1$ configuration and that the Fe≡N bond order is reduced to 2 owing to the presence of two unpaired electrons in the antibonding d_{xz} and d_{yz} orbitals. Recently, Meyer et al. [60] prepared the *trans*-$[N{\equiv}Fe(cyclam)N_3]^+$ ion via UV-photolysis of the corresponding diazido complex in frozen CH_3CN solution at 4 and 77 K and confirmed by ESR and Mössbauer spectroscopy that their nitrido complex also contains a high-spin Fe(V) atom.

Fig. 14 shows the Raman excitation profiles (REPs) of the ν(Fe≡N) vibration of N≡Fe(OEP) (upper part) and four vibrations of N_3–Fe(OEP) (lower part). It is seen that the REPs of all the four vibrations of the latter exhibit a large maximum in the Soret region near 400 nm and a second maximum near 500 nm. The fact that these REPs closely follow the electronic spectrum of N_3–Fe(OEP) suggests that they are resonance-enhanced via the π–π^* transition of the porphyrin. On the other hand, the REP of the ν(Fe≡N) vibration has a single maximum near 470 nm which is far from the porphyrin π–π^* transition. Thus, this mode is resonance-enhanced by the direct excitation of the Fe←N charge-transfer transition located near 470 nm.

As stated above, irradiation of N_3–Fe(OEP) with low power laser line at 488.0 nm yields N≡Fe(OEP). However, continued irradiation with high power laser line at 413.1 nm (near the Soret band) converts the nitrido complex to its μ-nitrido dimer $(Fe(OEP))_2N$. Traces A–C in Fig. 15 show the changes in the RR spectra during the first step. Traces D and E show the RR spectra obtained by continued irradiation with the 413.1 nm line at laser power of 10 and 220 mW, respectively. In trace E, it is seen that the ν(Fe≡N) band at 876 cm^{-1} disappears completely and a new set of bands having components at 798, 438 and 341 cm^{-1} emerges. The band at 438 cm^{-1} is upshifted by 6 cm^{-1} upon $^{NA}Fe/^{54}Fe$ substitution, but shows almost no shift

upon $^{14}N/^{15}N$ substitution. Thus, this band is assigned to the symmetric stretching vibration of the linear Fe–N–Fe bridge of the μ-nitrido dimer. Previously, Hofmann and Bocian [61] observed and assigned it at 439 cm^{-1} in the RR spectrum of $(Fe(OEP))_2N$ in CS_2 solution. The remaining bands at 798 and 341 cm^{-1} are attributed to the OEP vibrations of the μ-nitrido dimer.

Based on these observations, the following decomposition scheme has been proposed [58]:

$$N_3\text{–Fe(III)(OEP)} \xrightarrow{h\nu} N{\equiv}\text{Fe(V)(OEP)} \xrightarrow{\Delta} \text{(OEP)Fe(3.5)–N–Fe(3.5)(OEP)}$$

The critical laser power in the second step was found to be dependent on the thickness of the sample film which acts as a thermal insulator against the cooling head. Thus, step 2 proceeds via local heating which increases the contact of the nitrido complex with its decomposed product, Fe(OEP). Although the analogous TPP and TMP complexes exhibit ν(Fe≡N) at 876 and 873 cm^{-1}, respectively, they do not form the μ-nitrido dimer under the same conditions as that used for the OEP complex. This may be due the steric hindrance of the peripheral substituents of TPP and TMP that prevents the access of the two porphyrins.

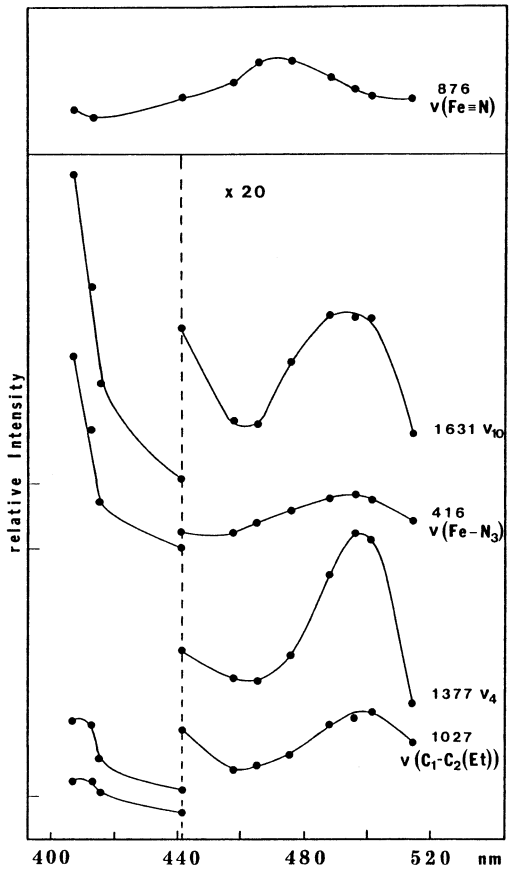

Fig. 14. Raman excitation profiles (REPs). Lower part: REPs of four vibrations of N_3–Fe(OEP) in CH_2Cl_2 solution at 176 K. Raman intensities with Q-band excitation are expanded by a factor of 20 as indicated. Upper part: REP of ν(Fe≡N) vibration of N≡Fe(OEP) formed by photolysis of N_3–Fe(OEP), thin film, ~30 K. Reproduced with permission from Ref. [58].

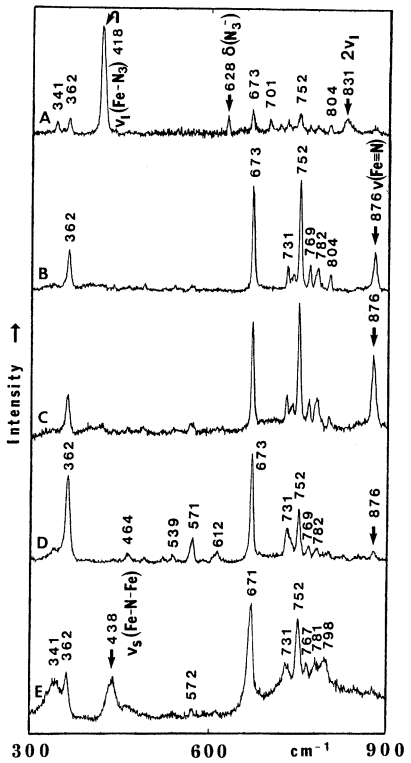

Fig. 15. RR spectra of N_3–Fe(OEP), thin film at 30 K, obtained from the same sample spot demonstrating spectral changes caused by laser irradiation. (A) 488.0 nm excitation, 5 mW; (B) 488.0 nm excitation, 60 mW, after 20 min of 488.0 nm, 60 mW irradiation; (C) 476.2 nm excitation, 60 mW; (D) 413.1 nm excitation, 10 mW; and (E) 413.1 nm excitation, 220 mW. Reproduced with permission from Ref. [58].

6. Summary and prospects

Panel a in Fig. 16 illustrates the bonding diagram originally proposed by Czernuszewicz et al. [62] to explain the abrupt drop in the ν(M=O) frequencies of metalloporphyrins in going from M = V(IV) (d^1), Cr(IV) (d^2) to Mn(IV) (d^3) and Fe(IV) (d^4) (trace b). The d electrons enter the non-bonding d_{xy} orbital in the first two complexes. In the latter two complexes, however, two d electrons enter the anti-bonding d_{xz} and d_{yz} orbitals, and this results in the reduction of the M–O bond order from 3 to 2. In the Mn(IV) complex, the d_{xy} orbital level is raised near the d_{xz} and d_{yz} orbitals due to special stability of the half-filled t_{2g} subshell, resulting in the high-spin $(d_{xy})^1(d_{xz})^1(d_{yz})^1$ configuration. As reflected on the ν(M=O) frequencies, the Fe=O bond order is higher than the Mn=O bond order since the effective nuclear charge of Fe(IV) is larger than that of Mn(IV).

Trace c shows a similar plot of the ν(M≡N) frequencies. Again, a sudden drop of the ν(M≡N) is observed in going from Cr(V)(d^1) and Mn(V)(d^2) to Fe(V)(d^3), and this result can be explained using the same bonding scheme as shown in panel a. Thus, a simple formulation as Fe(V)≡N is misleading since it is essentially a double bond.

Fig. 17 illustrates the speculative extensions of the present laser photolysis technique for the preparation of Co(IV,V) and Ni(IV,V) porphyrins. Complexes such as O=Co(IV)(por) and O=Ni(IV)(por) may be prepared by the O–O bond cleavage of the corresponding dioxygen adducts in O_2 matrices at 10–30 K. Dioxygen adducts of Co(II) porphyrins are well-known as the model compounds of oxy–heme proteins, and their RR spectra have been studied extensively. Although dioxygen adducts of Ni(II) porphyrins are not known, it may be possible to stabilize them in O_2 matrices. Examples of the Ni(IV) state are found in the $[NiF_6]^{2-}$ and $[Ni(dias)_2Br_2]^{2+}$ ions. Nitrido complexes such as N≡Co(V)(por) and N≡Ni(V)(por) may be prepared by laser photolysis of the corresponding azido complexes in thin films at 10–30 K. To date, the Co(V) state is known for the $[CoO_4]^{3-}$ ion although no reports are yet available for the Ni(V) state. It may be possible to prepare these highly unstable complexes if proper experimental conditions are chosen.

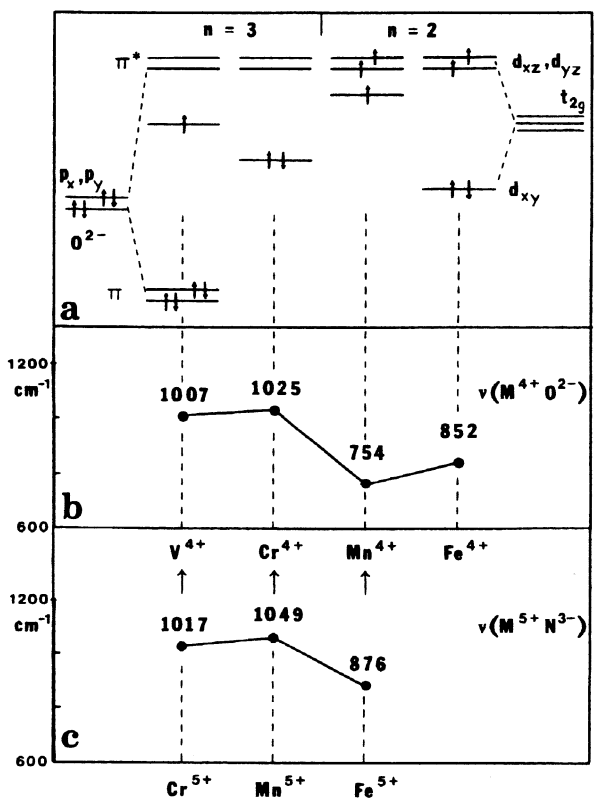

Fig. 16. (a) Simple MO diagram of $M^{4+}O^{2-}$ moiety. Only dπ–pπ interactions are shown [54]. (b) Variation of ν(M=O) in $M^{4+}O^{2-}$ porphyrins. Observed frequencies are indicated for M = V, Cr, Mn and Fe [49]. (c) Variation of ν(M≡N) in $M^{5+}N^{3-}$ porphyrins. Observed frequencies are shown for M = Cr, Mn and Fe. Reproduced with permission from Ref. [57].

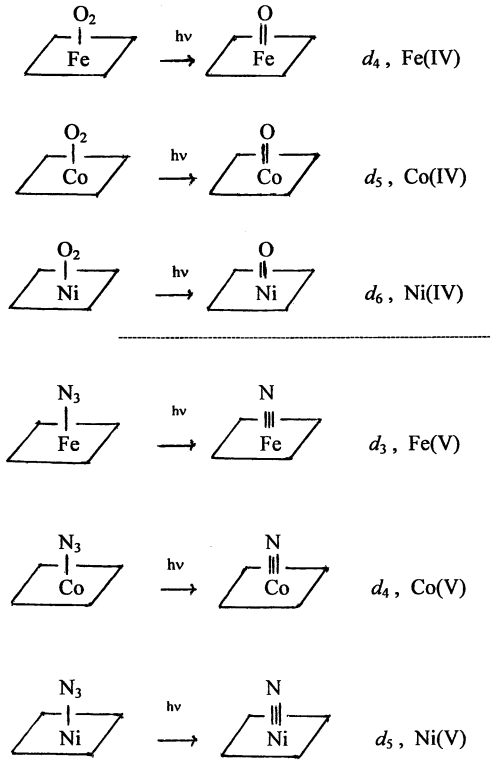

Fig. 17. Possible extension of the laser photolysis technique to cobalt and nickel porphyrins.

Acknowledgements

The author wishes to express his sincere thanks to all his collaborators who participated in the work described in this review and to Professor J.R. Kincaid of the Marquette University for his valuable comments.

References

[1] K. Nakamoto, Coord. Chem. Rev. 100 (1990) 363.
[2] J.R. Kincaid, in: K.M. Kadish, K.M. Smith, R. Guilard (Eds.), Resonance Raman Spectra of Heme Proteins and Model Compounds. In: The Porphyrin Handbook, vol. 7, Academic Press, New York, 2000, p. 225.
[3] T. Kitagawa, Y. Mizutani, Coord. Chem. Rev. 135–136 (1994) 685.
[4] T. Kitagawa, in: R.J.H. Clark, R.E. Hester (Eds.), Resonance Raman Spectra of Reaction Intermediates of Heme Enzymes. In: Spectroscopy of Biological Systems, vol. 13, Wiley, New York, 1986, p. 443.
[5] E.W. Svastits, J.H. Dawson, R. Breslow, S.H. Gellman, J. Am. Chem. Soc. 107 (1985) 6427.
[6] J.H. Dawson, M. Sono, Chem. Rev. 87 (1987) 1255.
[7] K. Bajdor, K. Nakamoto, J. Am. Chem. Soc. 106 (1984) 3045.
[8] W. Scheuermann, K. Nakamoto, Appl. Spectrosc. 32 (1978) 251.

[9] L.M. Proniewicz, I.R. Paeng, K. Nakamoto, J. Am. Chem. Soc. 113 (1991) 3294.
[10] T. Watanabe, T. Ama, K. Nakamoto, J. Phys. Chem. 88 (1984) 440.
[11] L.M. Proniewicz, K. Bajdor, K. Nakamoto, J. Phys. Chem. 90 (1986) 1760.
[12] A. Weselucha-Birczynska, I.R. Paeng, A.A. Shabana, K. Nakamoto, N. J. Chem. 16 (1992) 563.
[13] D.-H. Chin, G.N. LaMar, A.L. Balch, J. Am. Chem. Soc. 102 (1980) 4344.
[14] A.L. Balch, Y.-W. Chan, R.-J. Cheng, G.N. LaMar, L. Latos-Grazynski, M.W. Renner, J. Am. Chem. Soc. 106 (1984) 7779.
[15] I.R. Paeng, H. Shiwaku, K. Nakamoto, J. Am. Chem. Soc. 110 (1988) 1995.
[16] K. Nakamoto, Y. Nonaka, T. Ishiguro, M.W. Urban, M. Suzuki, M. Kozuka, Y. Nishida, S. Kida, J. Am. Chem. Soc. 104 (1982) 3386.
[17] Y. Mizutani, S. Hashimoto, Y. Tatsuno, T. Kitagawa, J. Am. Chem. Soc. 112 (1990) 6809.
[18] K. Czarnecki, L.M. Proniewicz, H. Fujii, J.R. Kincaid, J. Am. Chem. Soc. 118 (1996) 4680.
[19] R.S. Czernuszewicz, K.A. Macor, J. Raman Spectrosc. 19 (1988) 553.
[20] P.K. Shantha, A.L. Verma, Inorg. Chem. 35 (1996) 2723.
[21] G.N. La Mar, J.S. de Ropp, L. Latos-Grazynski, A.L. Balch, R.B. Johnson, K.M. Smith, D.W. Parish, R.-J. Cheng, J. Am. Chem. Soc. 105 (1983) 782.
[22] M. Schappacher, G. Chottard, R. Weiss, J. Chem. Soc. Chem. Commun. (1986) 93.
[23] R.T. Kean, W.A. Oertling, G.T. Babcock, J. Am. Chem. Soc. 109 (1987) 2185.
[24] W.A. Oertling, R.T. Kean, R. Weber, G.T. Babcock, Inorg. Chem. 29 (1990) 2633.
[25] A. Gold, K. Jayaraj, P. Doppelt, R. Weiss, G. Chottard, E. Bill, X. Ding, A.X. Trautwein, J. Am. Chem. Soc. 110 (1988) 5756.
[26] K.R. Rodgers, C.A. Reed, Y.O. Su, T.G. Spiro, Inorg. Chem. 31 (1992) 2688.
[27] S. Hashimoto, Y. Tatsuno, T. Kitagawa, Proc. Jpn. Acad. Ser. B 60 (1984) 345.
[28] S. Hashimoto, Y. Tatsuno, T. Kitagawa, Proc. Natl. Acad. Sci. USA 83 (1986) 2417.
[29] S. Hashimoto, R. Nakajima, I. Yamazaki, Y. Tatsuno, T. Kitagawa, FEBS Lett. 208 (1986) 305.
[30] J. Terner, A.J. Sitter, C.M. Reczek, Biochim. Biophys. Acta 828 (1985) 73.
[31] A.J. Sitter, C.M. Reczek, J. Terner, J. Biol. Chem. 260 (1985) 7515.
[32] S. Hashimoto, J. Teraoka, T. Inubushi, T. Yonetani, T. Kitagawa, J. Biol. Chem. 261 (1986) 11110.
[33] C.M. Reczek, A.J. Sitter, J. Terner, J. Mol. Struct. 214 (1989) 27.
[34] W.A. Oertling, H. Hoogland, G.T. Babcock, R. Wever, Biochemistry 27 (1988) 5395.
[35] T. Egawa, H. Miki, T. Ogura, R. Makino, Y. Ishimura, T. Kitagawa, FEBS Lett. 305 (1991) 206.
[36] C.M. Hosten, A.M. Sullivan, V. Palaniappan, M.M. Fitzgerald, J. Terner, J. Biol. Chem. 269 (1994) 13966.
[37] W.-J. Chuang, J. Heldt, H.E. Van Wart, J. Biol. Chem. 264 (1989) 14209.
[38] D.A. Proshlyakov, T. Ogura, K. Shinzawa-Itoh, S. Yoshikawa, T. Kitagawa, Biochemistry 35 (1996) 76.
[39] M.A. Kahlow, T.M. Zuberi, R.B. Gennis, T.M. Loehr, Biochemistry 30 (1991) 11485.
[40] A.J. Sitter, C.M. Reczek, J. Terner, Biochim. Biophys. Acta 828 (1985) 229.
[41] J.T. Groves, R.C. Haushalter, M. Nakamura, T.E. Nemo, B.J. Evans, J. Am. Chem. Soc. 103 (1981) 2884.
[42] J.R. Kincaid, A.J. Schneider, K.-J. Paeng, J. Am. Chem. Soc. 111 (1989) 735.
[43] S. Hashimoto, Y. Tatsuno, T. Kitagawa, J. Am. Chem. Soc. 109 (1987) 8096.
[44] S. Hashimoto, Y. Mizutani, Y. Tatsuno, T. Kitagawa, J. Am. Chem. Soc. 113 (1991) 6542.
[45] K. Czarnecki, S. Nimri, Z. Gross, L.M. Proniewicz, J.R. Kincaid, J. Am. Chem. Soc. 118 (1996) 2929.
[46] R.S. Czernuszewicz, K.A. Macor, X.-Y. Li, J.R. Kincaid, T.G. Spiro, J. Am. Chem. Soc. 111 (1989) 3860.
[47] H. Fujii, K. Ichikawa, Inorg. Chem. 31 (1992) 1110.
[48] K. Ayougou, D. Mandon, J. Fischer, R. Weiss, M. Muether, V. Schuenemann, A.X. Trautwein, E. Bill, J. Terner, Chem. Eur. J. 2 (1996) 1159.
[49] K. Jayaraj, J. Terner, A. Gold, D.A. Roberts, R.N. Austin, D. Mandon, R. Weiss, E. Bill, M. Muether, A.X. Trautwein, Inorg. Chem. 35 (1996) 1632.
[50] (a) T. Ogura, T. Kitagawa, J. Am. Chem. Soc. 109 (1987) 2177; (b) T. Ogura, T. Kitagawa, Rev. Sci. Instrum. 59 (1988) 1316.
[51] W.A. Oertling, G.T. Babcock, Biochemistry 27 (1988) 3331.
[52] K.-J. Paeng, J.R. Kincaid, J. Am. Chem. Soc. 110 (1988) 7913.
[53] W.-J. Chuang, H.E. Van Wart, J. Biol. Chem. 267 (1992) 13293.
[54] V. Palaniappan, J. Terner, J. Biol. Chem. 264 (1989) 16046.
[55] J.R. Kincaid, Y. Zheng, J. Al-Mustafa, K. Czarnecki, J. Biol. Chem. 271 (1996) 2880.
[56] J.T. Groves, T. Takahashi, J. Am. Chem. Soc. 105 (1983) 2073.
[57] W.-D. Wagner, K. Nakamoto, J. Am. Chem. Soc. 110 (1988) 4044.
[58] W.-D. Wagner, K. Nakamoto, J. Am. Chem. Soc. 111 (1989) 1590.
[59] R.S. Czernuszewicz, W.-D. Wagner, G.B. Ray, K. Nakamoto, J. Mol. Struct. 242 (1991) 99.
[60] K. Meyer, E. Bill, B. Mienert, T. Weyhermuller, K. Wieghardt, J. Am. Chem. Soc. 121 (1999) 4859.
[61] J.A. Hofmann Jr., D.F. Bocian, J. Phys. Chem. 88 (1984) 1472.
[62] R.S. Czernuszewicz, Y.O. Su, M.K. Stern, K.A. Macor, D. Kim, J.T. Groves, T.G. Spiro, J. Am. Chem. Soc. 110 (1988) 4158.